

## Supporting Information

### Template free protocol for fabrication of Ni(II)-loaded magnetically separable nanoreactor scaffold for confined synthesis of unsymmetrical diaryl sulfides in water

Gunjan Arora,<sup>a</sup> Manavi Yadav,<sup>a,b</sup> Rashmi Gaur,<sup>a</sup> Radhika Gupta,<sup>a</sup> Pooja Rana,<sup>a</sup> Priya Yadav<sup>a,b</sup> and Rakesh K. Sharma<sup>a\*</sup>

<sup>a</sup>Green Chemistry Network Centre, Department of Chemistry, University of Delhi, Delhi-110007, India

<sup>b</sup>Department of Chemistry, Hindu College, University of Delhi, Delhi-110007, India

#### Details of Materials, reagents and instruments used

Ferric chloride hexahydrate, trisodium citrate, sodium acetate and nickel acetate were obtained from Thomas Baker. Resorcinol was purchased from Central Drug House. Ethylene glycol, diethylene glycol, and formaldehyde were acquired from Spectrochem. Ethanol, ethyl acetate, and liquid ammonia (30%) were procured from Fisher Scientific. All the other reagents were of analytical grade and used without purification. Double deionized water was used during the entire study.

#### Instrumentation

The Fourier transform-infrared spectra (FT-IR) were documented on PerkinElmer Spectrum 2000 with a scanning range of 400-4000  $\text{cm}^{-1}$ . X-ray diffraction (XRD) spectra were recorded on D8 Advance (Karlsruhe, bundesland, Germany) diffractometer in the  $2\theta$  range of  $15-90^\circ$  with scanning rate of  $4^\circ \text{ min}^{-1}$  ( $K\alpha$ ;  $\lambda = 1.5406 \text{ \AA}$ ). The size and morphology of the catalyst was determined using FEI TECHNAI G<sup>2</sup> T20 transmission electron microscope operated at 200 kV. The powered samples were dispersed in ethanol and drop casted over a copper grid coated with an amorphous carbon film. Particle size was analysed using "ImageJ" software. Field emission-scanning electron microscopic analysis (FE-SEM) and Scanning electron microscopic analysis (SEM) were operated on Digital Scanning Electron Microscope - JSM 6100 (JEOL) and JEOL, JSM 6610LV microscope respectively. For this, powdered material was transferred to a metal stub covered with carbon tape which was sputter-coated with a JEOL JEC-3000 FC auto fine coater platinum sputtering machine. Ametek EDAX system was used to investigate the chemical composition of the elements through energy dispersive X-ray spectroscopic (EDX) analysis. The quantitative analysis of metal content in the catalyst was estimated by using Inductively coupled plasma-mass spectroscopy (ICP-MS, PerkinElmer Optima 2100 DV). Magnetization measurements were carried out using vibrating sample magnetometer (EV-9, Microsense, ADE). In order to determine the oxidation state of palladium present in the synthesized catalyst, X-ray photoelectron spectroscopic (XPS) studies were done on a K-Alpha<sup>TM</sup> X-ray photoelectron spectrometer. The analysis of the final products was done using Agilent gas chromatograph (6850 GC) with a HP-5MS 5% phenyl methyl siloxane capillary column ( $30.0 \text{ m} \times 0.25 \text{ mm} \times 0.25 \mu\text{m}$ ) and a quadrupole mass filter equipped 5975 mass selective detector (MSD) with helium as a carrier gas.

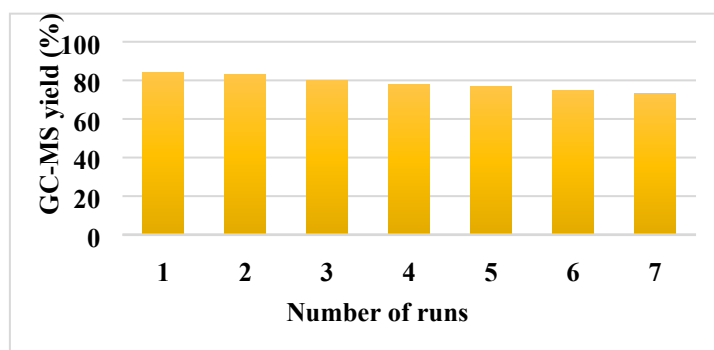


**Figure S1.** Reusability of the catalyst. Reaction conditions: 4-cyanophenylhydrazine hydrochloride (1 mmol), 4-bromothiol (1 mmol),  $\text{K}_2\text{CO}_3$  (3 equiv),  $\text{Ni}@ \text{Fe}_3\text{O}_4\text{-C}$  catalyst (25 mg),  $\text{H}_2\text{O}$  (3 mL), rt, 20 h.

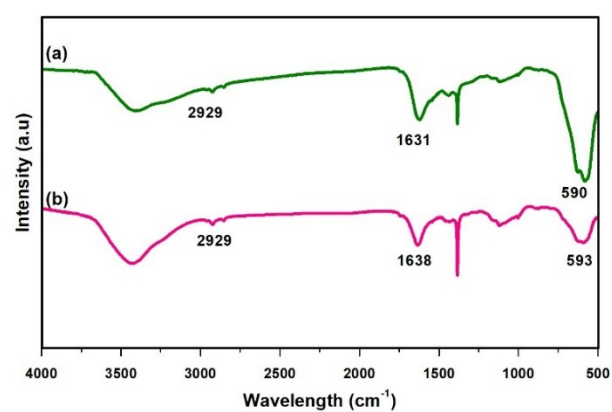


**Figure S2.** FT-IR curves of Ni@Fe<sub>3</sub>O<sub>4</sub>-C a) Fresh and b) after 7th run.

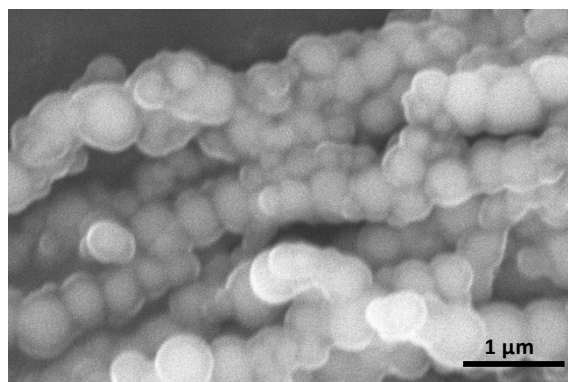


**Figure S3.** SEM image of recovered Ni@Fe<sub>3</sub>O<sub>4</sub>-C after 7th run.

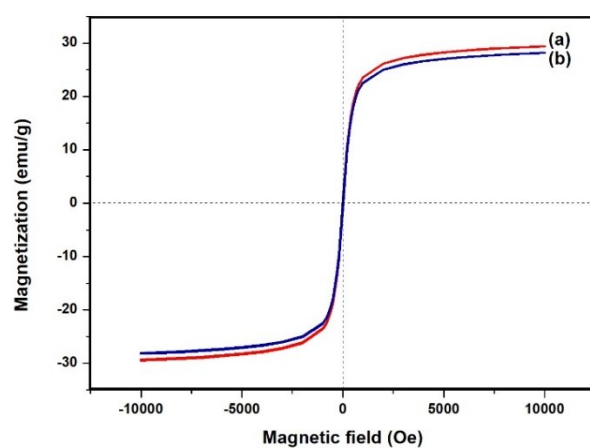
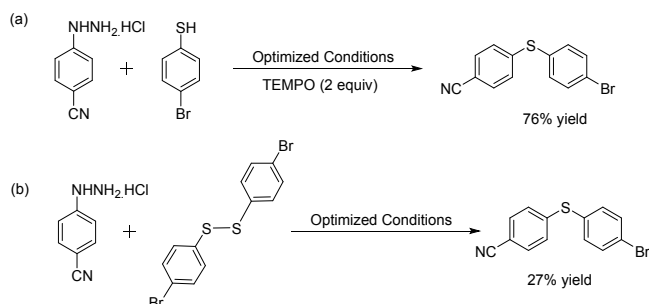


**Figure S4.** VSM curves of Ni@Fe<sub>3</sub>O<sub>4</sub>-C a) Fresh and b) after 7th run.

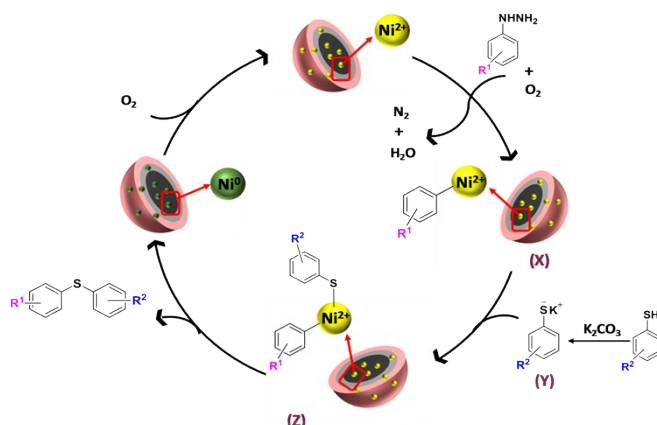
## Proposed mechanism

To elucidate a possible mechanistic pathway for the cross-coupling reaction of arylhydrazines and disulfides, some experiments were performed (**Scheme S1**). When standard reaction was conducted in the presence of radical scavenger, 2,2,6,6-tetramethylpiperidine-1-oxyl (TEMPO), 76% of the desired product was formed (**Scheme S1a**). Since the reaction efficiency remained nearly intact, it is clear that radical intermediates are not involved in the reaction. Further to check the formation of disulfide as intermediate during the reaction course, standard reaction was performed with 1,2-bis(4-bromophenyl)-disulfane as a starting reagent in place of 4-bromobenzenethiol (**Scheme S1b**). Significantly lower yield of product excludes any possibility of disulfide formation.



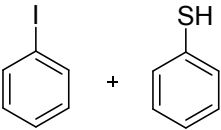
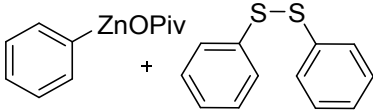
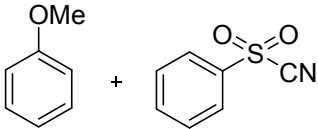
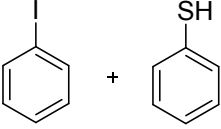
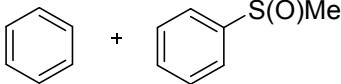
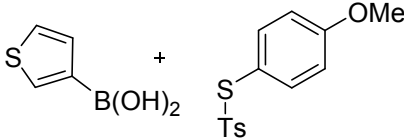
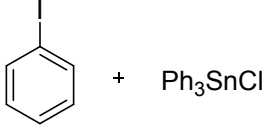
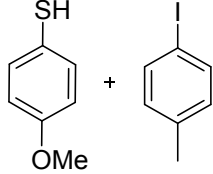
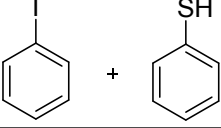
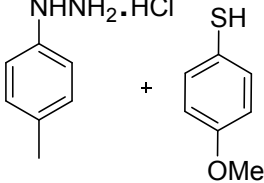
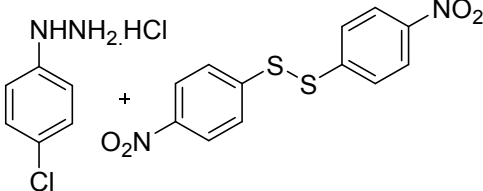
**Scheme S1.** Control experiments.

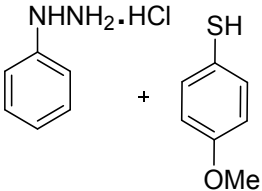
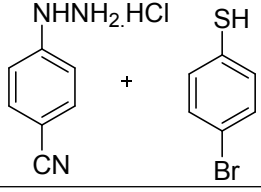
Based on these studies and literature,<sup>1</sup> we proposed a plausible reaction mechanism (**Scheme S2**) for the Ni@Fe<sub>3</sub>O<sub>4</sub>-C catalyzed oxidative cross-coupling reaction of arylhydrazines with arenethiols to form diaryl sulfides. Reaction begins with the nickel catalyzed cleavage of C-N bond of arylhydrazine to form aryl nickel species (**X**) along with nitrogen gas and water as by-products. Simultaneously, arenethiol reacts with K<sub>2</sub>CO<sub>3</sub> to form benzenethiolate intermediate (**Y**). Next, transmetalation of species (**X**) with intermediate (**Y**) forms the active nickel species (**Z**) which undergoes reductive elimination to form desired diaryl sulfide and Ni (0) species.<sup>1</sup> The generated Ni (0) species is re-oxidized to Ni (II) catalyst by molecular oxygen present in air, thus completes the catalytic cycle and regenerates the catalyst.



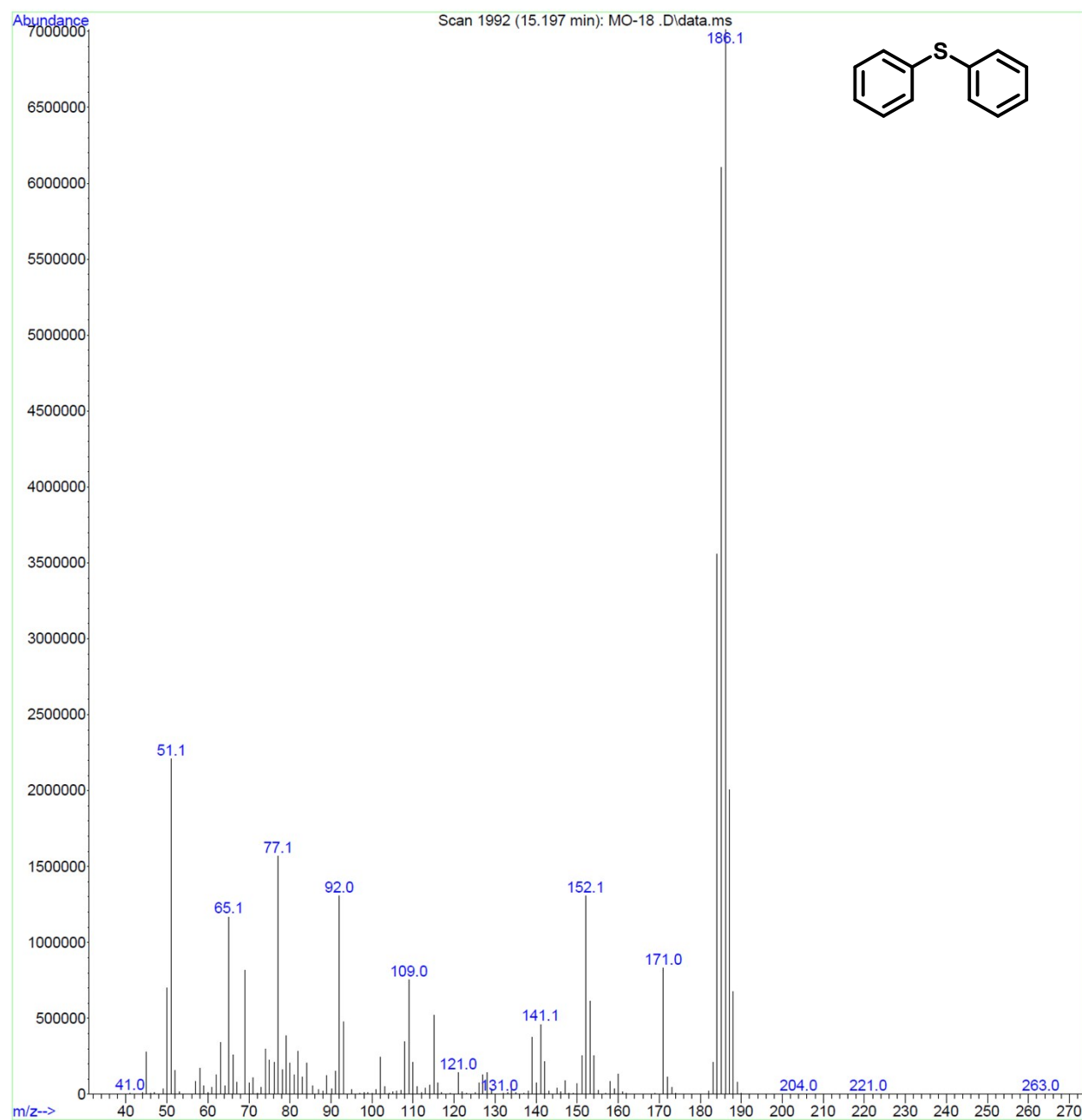
**Scheme S2.** Plausible reaction mechanism for the Ni@Fe<sub>3</sub>O<sub>4</sub>-C catalyzed synthesis of diaryl sulfides.

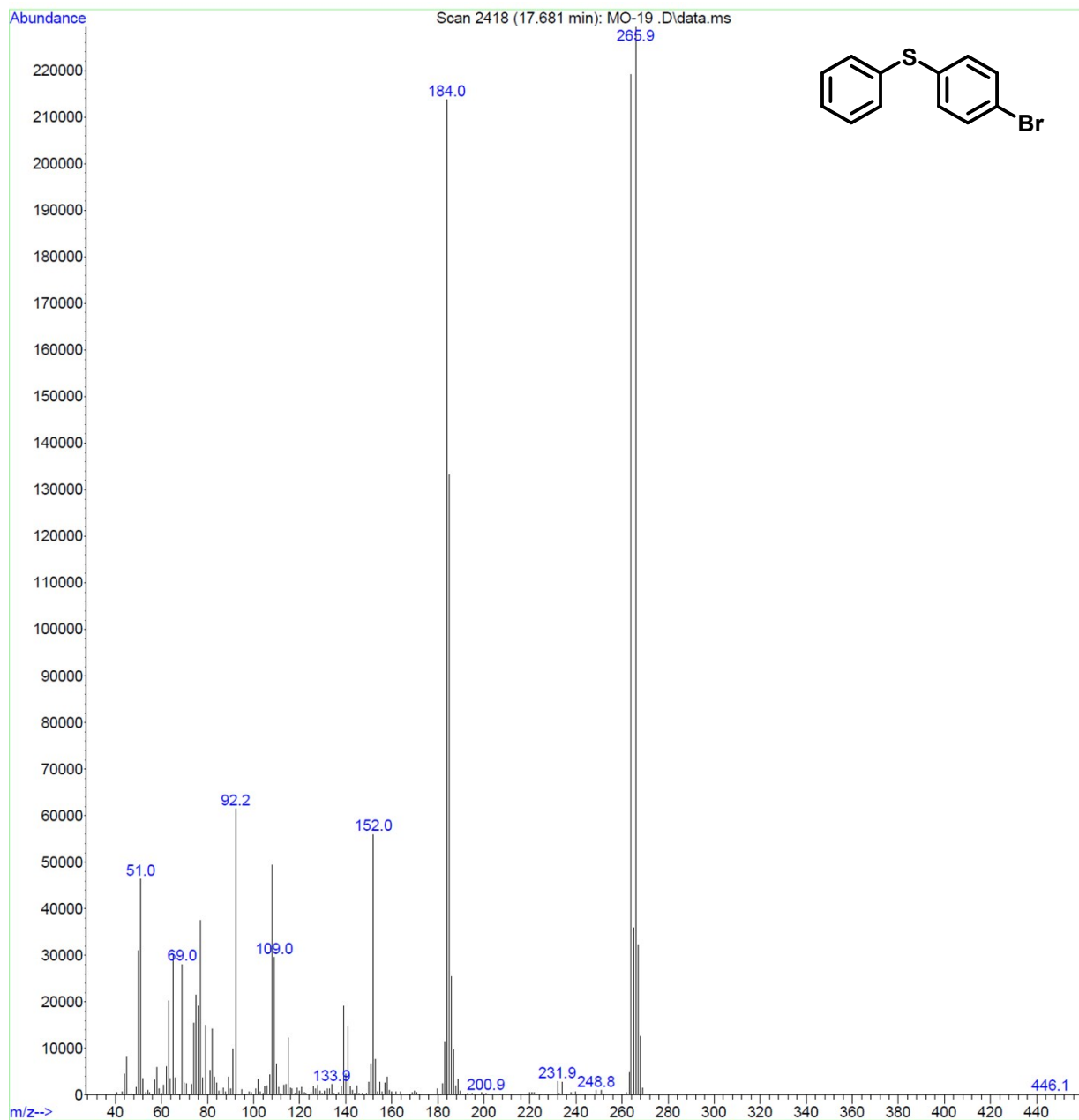
**Table S1.** Comparison of the catalytic activity of the Ni@Fe<sub>3</sub>O<sub>4</sub>-C catalyst with other previously reported catalysts for the synthesis of diaryl sulfides.

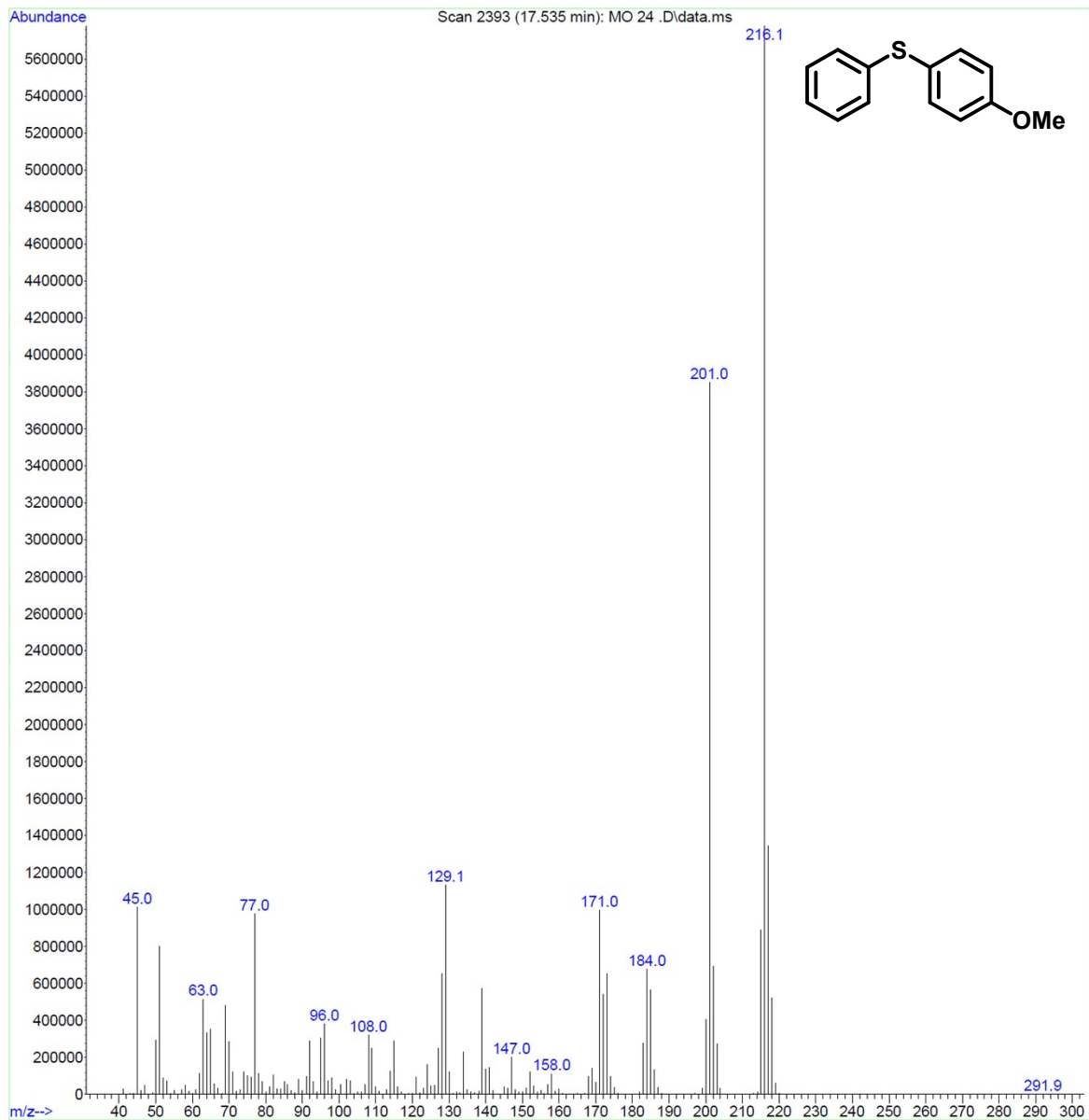
Entry	Reactants	Reaction Conditions	Yield (%)	Reference
1		10 mol% Ni(OAc) <sub>2</sub> , 5 mol% IPr, KO <sup>t</sup> Bu DMF, 70 °C, 12 h	92	<sup>2</sup>
2		CoCl <sub>2</sub> (10 mol%), THF, rt, 12 h	78	<sup>3</sup>
3		Pd(OAc) <sub>2</sub> , CF <sub>3</sub> COOH, rt, 1 h	41	<sup>4</sup>
4		Nano-CuFe <sub>2</sub> O <sub>4</sub> (5 mol%), Cs <sub>2</sub> CO <sub>3</sub> (1.0 equiv), DMSO (2.0 mL), N <sub>2</sub> , 100 °C, 24 h	98	<sup>5</sup>
5		(i) Tf <sub>2</sub> O (1.1 equiv), CH <sub>2</sub> Cl <sub>2</sub> (ii) DBU	50	<sup>6</sup>
6		[Rh(OH)(cod)] <sub>2</sub> (2.5 mol%), K <sub>3</sub> PO <sub>4</sub> (2.0 equiv), MeOH, 50 °C, 24 h	91	<sup>7</sup>
7		NiFe <sub>2</sub> O <sub>4</sub> MNPs (29 mol%), KF (3 mmol), S <sub>8</sub> (1.5 mmol), K <sub>2</sub> CO <sub>3</sub> (4 mmol), H <sub>2</sub> O, Bu <sub>4</sub> NOH (1 mmol), 60 °C	95	<sup>8</sup>
8		Ir[dF(CF <sub>3</sub> )ppy] <sub>2</sub> (dtbbpy)PF <sub>6</sub> (2 mol%), NiCl <sub>2</sub> ·glyme (10 mol%), dtbbpy (15 mol%), pyridine (2 equiv), MeCN, 34 W blue LED, rt, 24 h	93	<sup>9</sup>
9		In(OTf) <sub>3</sub> (10 mol%), TMEDA (20 mol%), KOH (2.0 equiv), DMSO, 135 °C, 24 h, N <sub>2</sub> atmosphere	96	<sup>10</sup>
10		Cu(NO <sub>3</sub> ) <sub>2</sub> ·3H <sub>2</sub> O, PEG-functionalized nitrogen ligand, Cs <sub>2</sub> CO <sub>3</sub> , O <sub>2</sub> , H <sub>2</sub> O, 100 °C, 12 h	92	<sup>11</sup>
11		CsCO <sub>3</sub> (1 equiv), DMSO, 25 °C, 24 h, under air	82	<sup>12</sup>

12		Pd(OAc) <sub>2</sub> (5 mol %), PCy <sub>3</sub> (10 mol %), Na <sub>2</sub> CO <sub>3</sub> (0.4 mmol), PhMe (2.0 mL), O <sub>2</sub> balloon, 100 °C, 12 h	82	<sup>1</sup>
13		Ni@Fe <sub>3</sub> O <sub>4</sub> -C (25 mg), K <sub>2</sub> CO <sub>3</sub> (3 equiv), H <sub>2</sub> O, rt, 20 h, under air	84	Present work

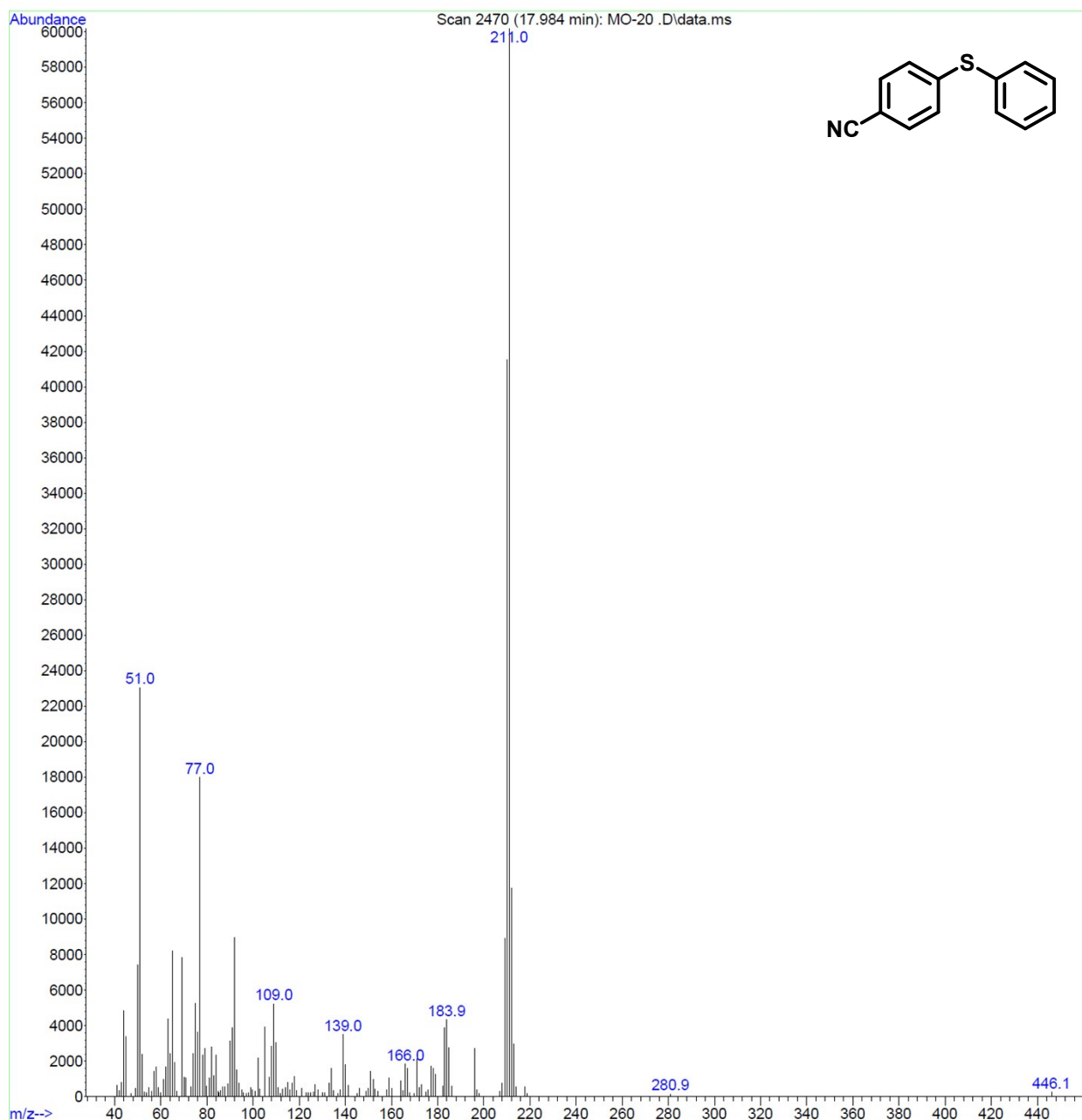
## GC-MS Spectra of Products

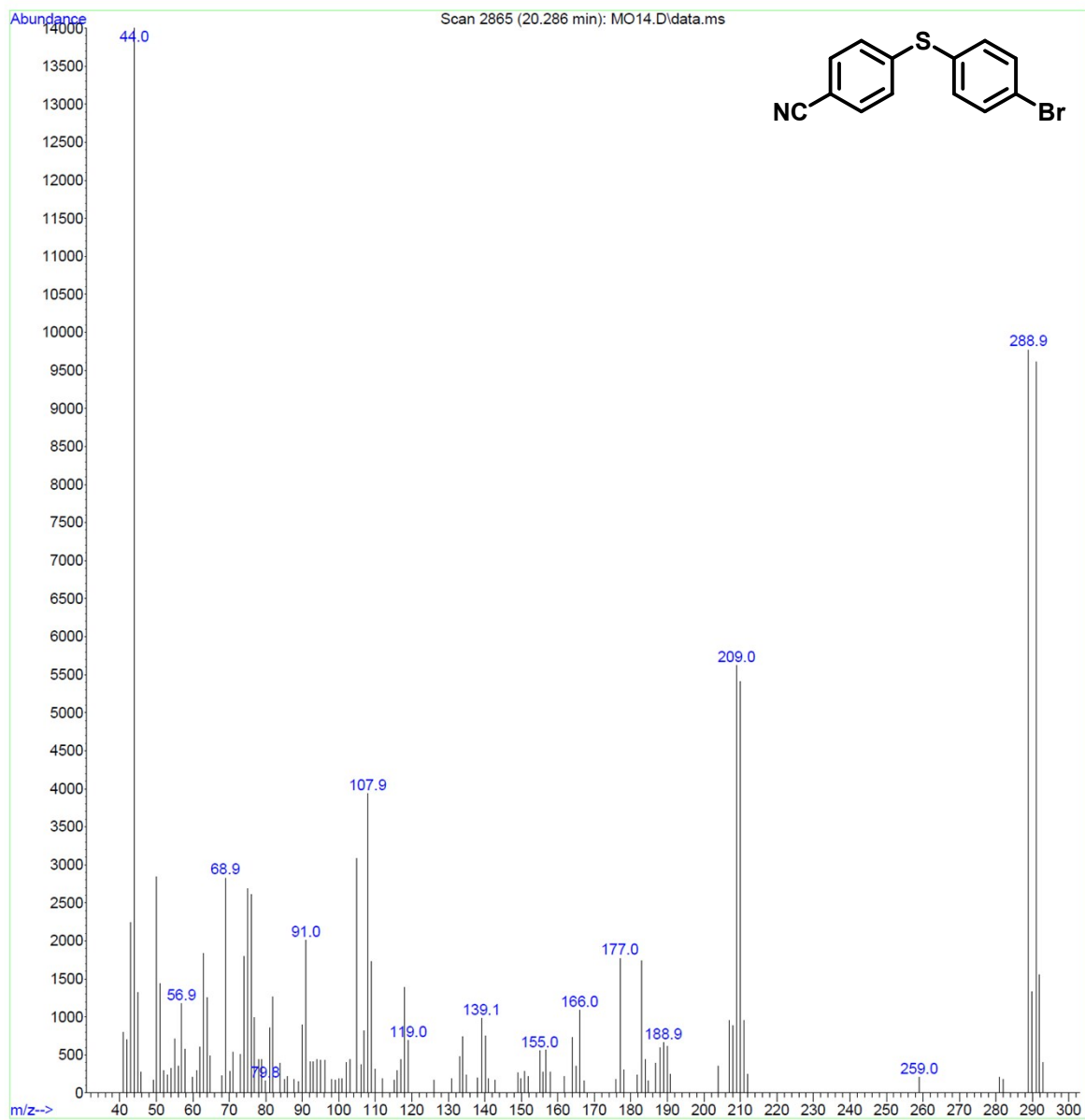


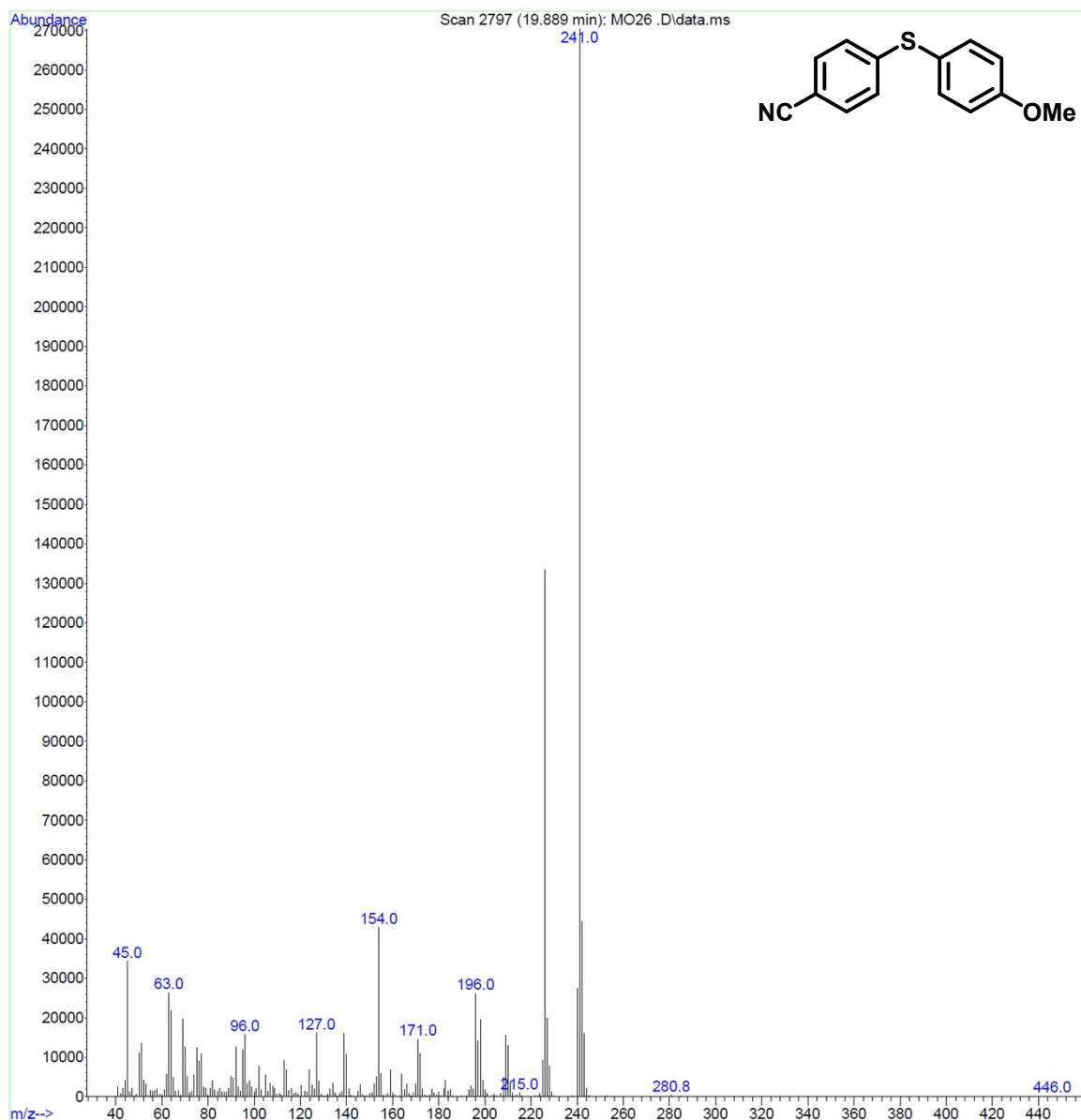


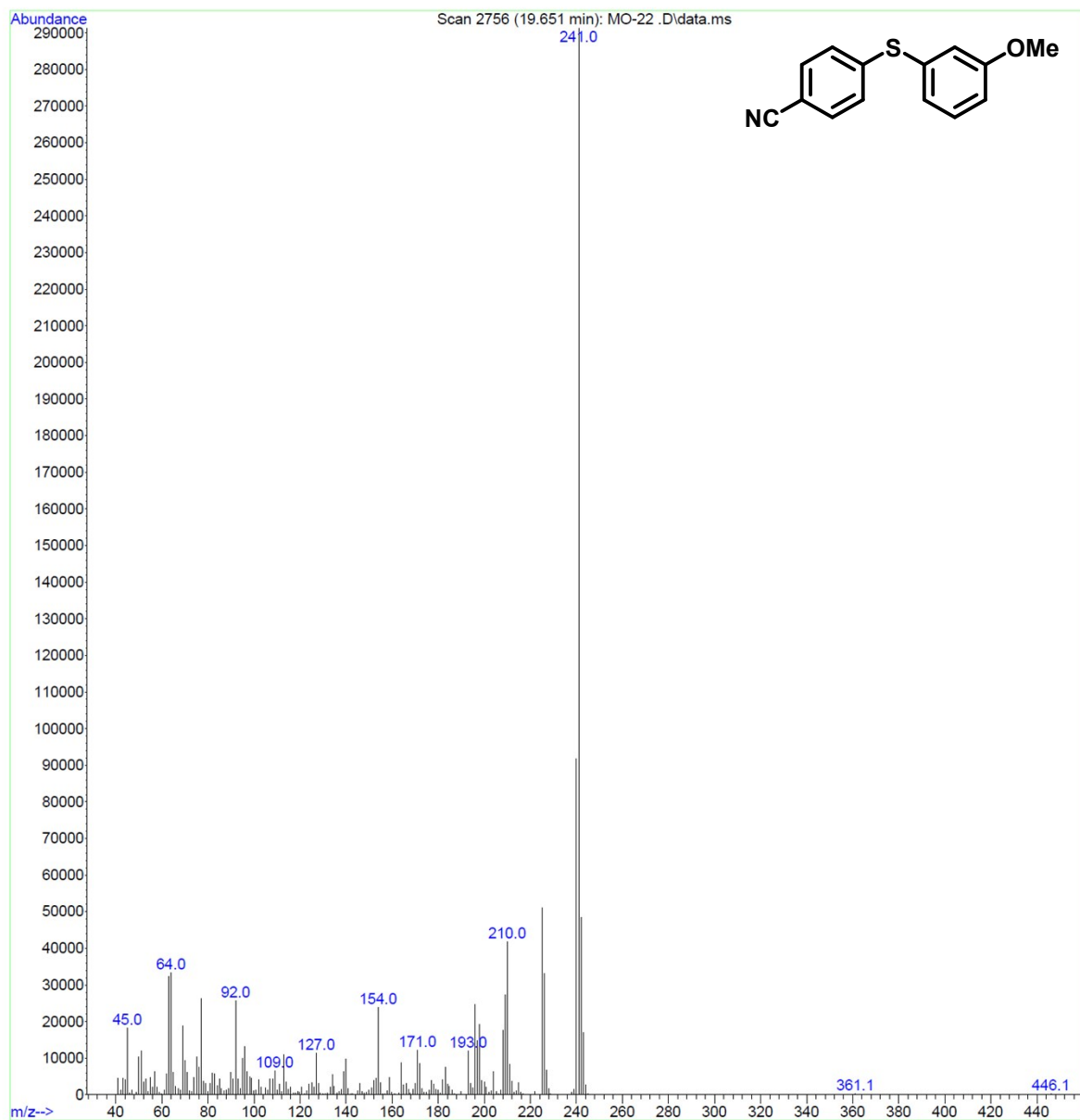


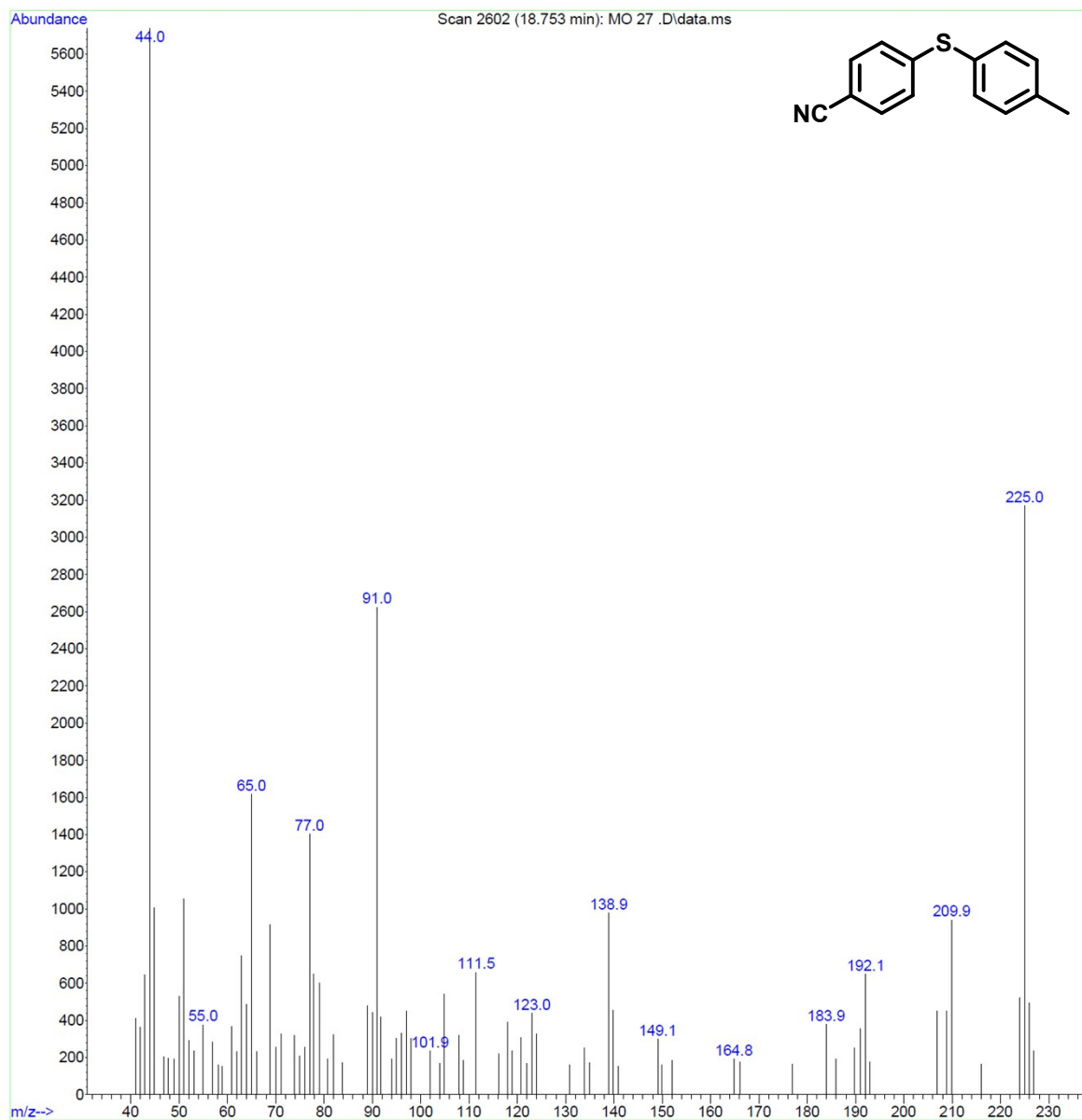


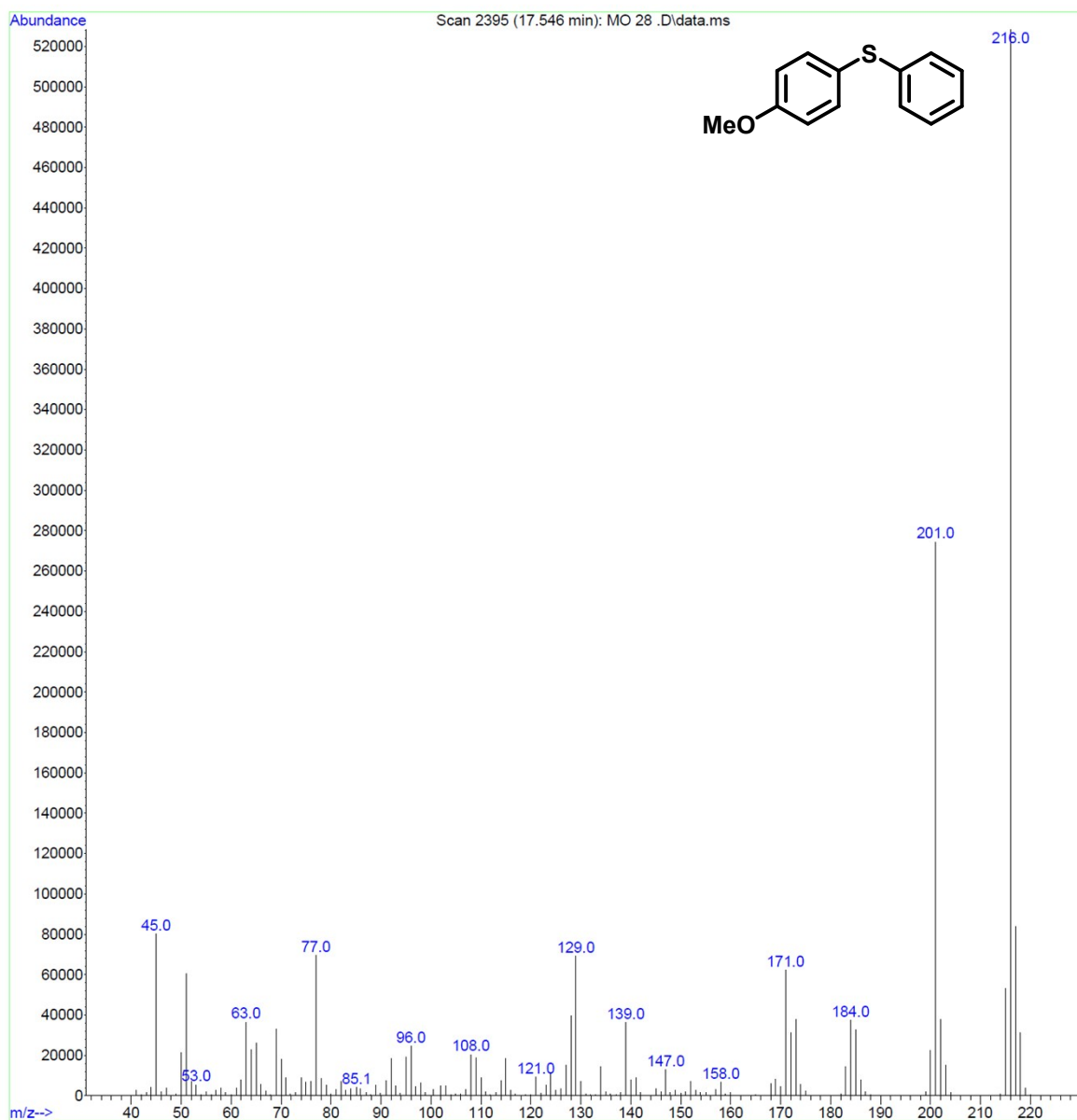


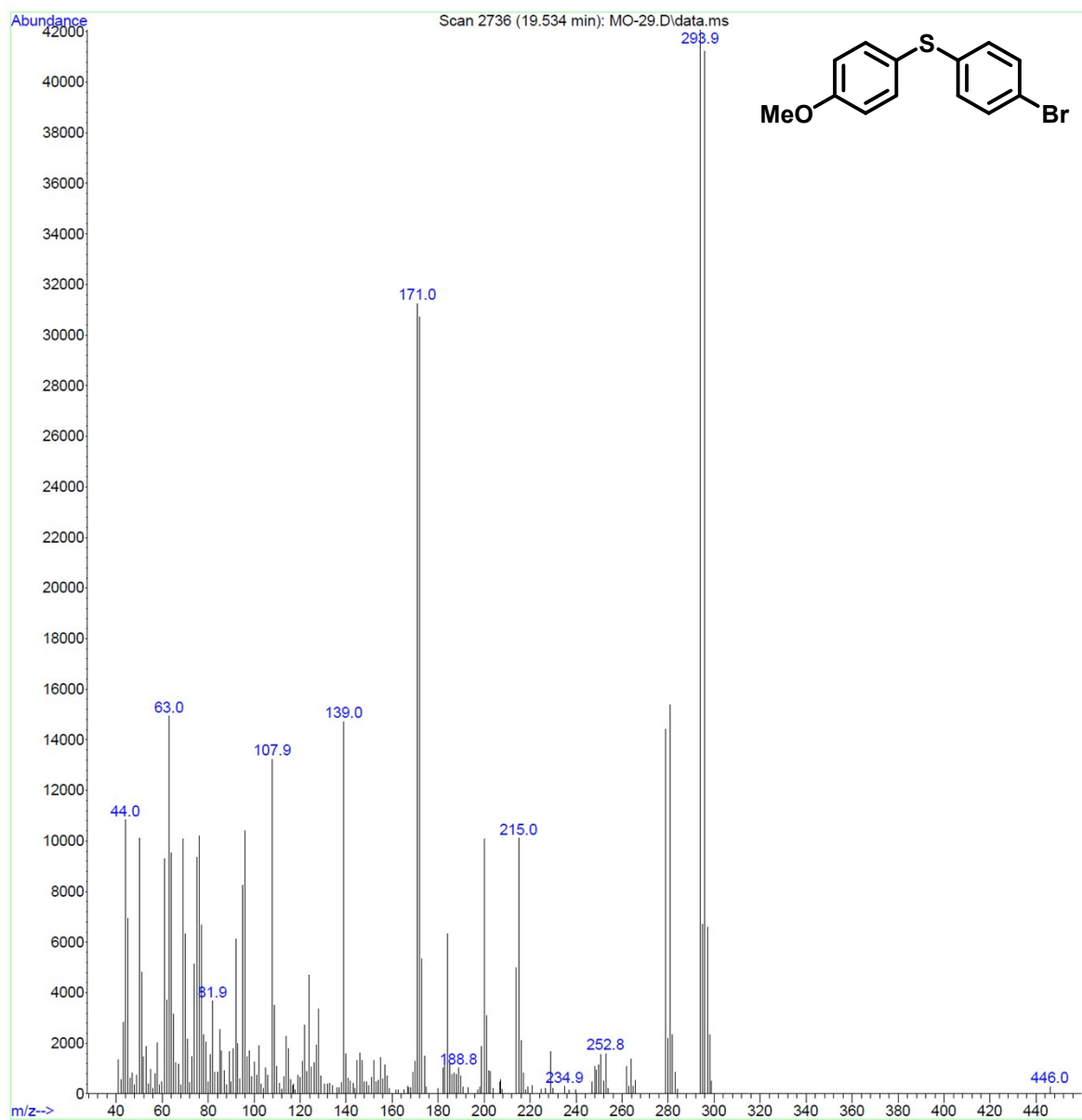


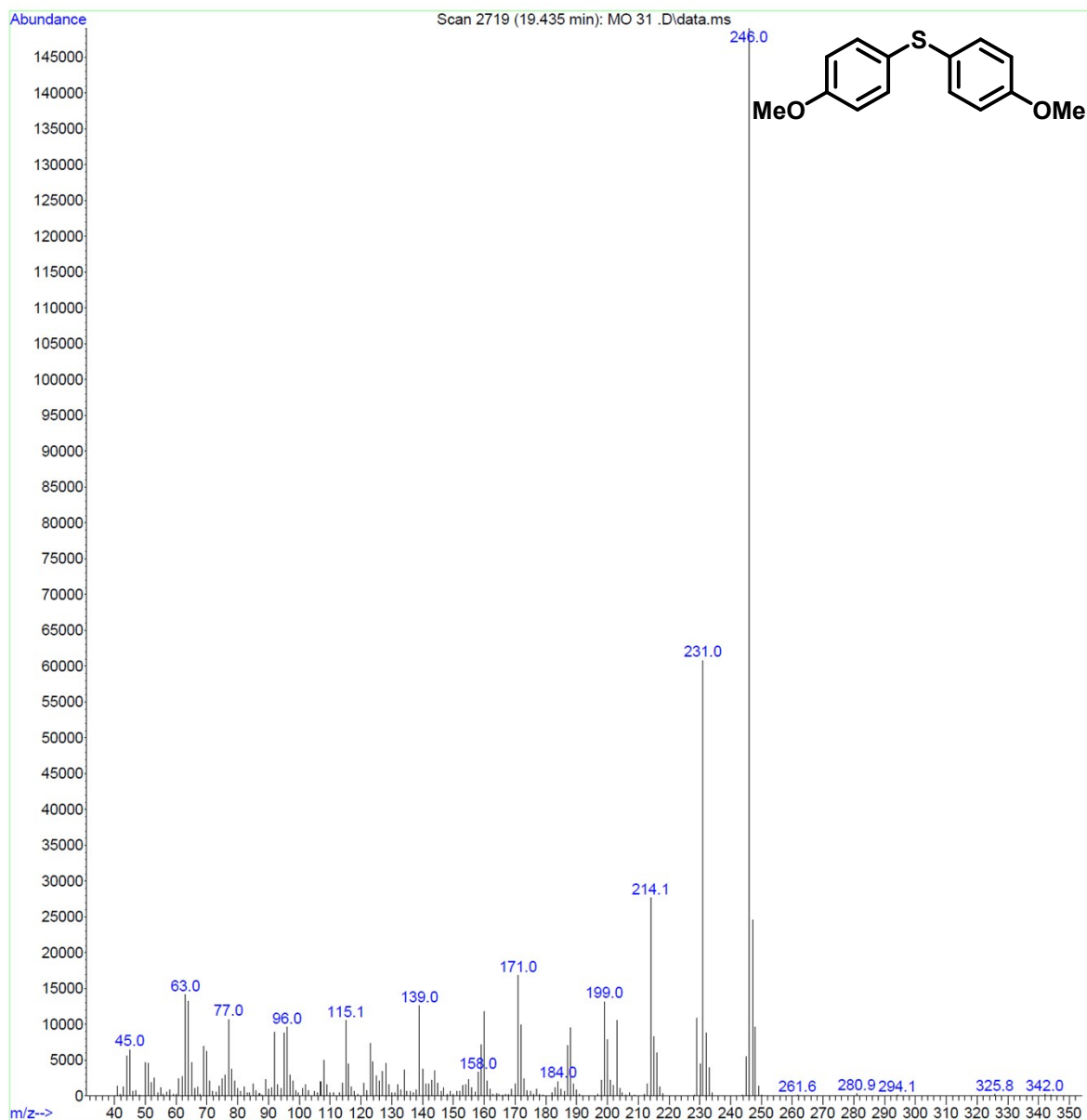




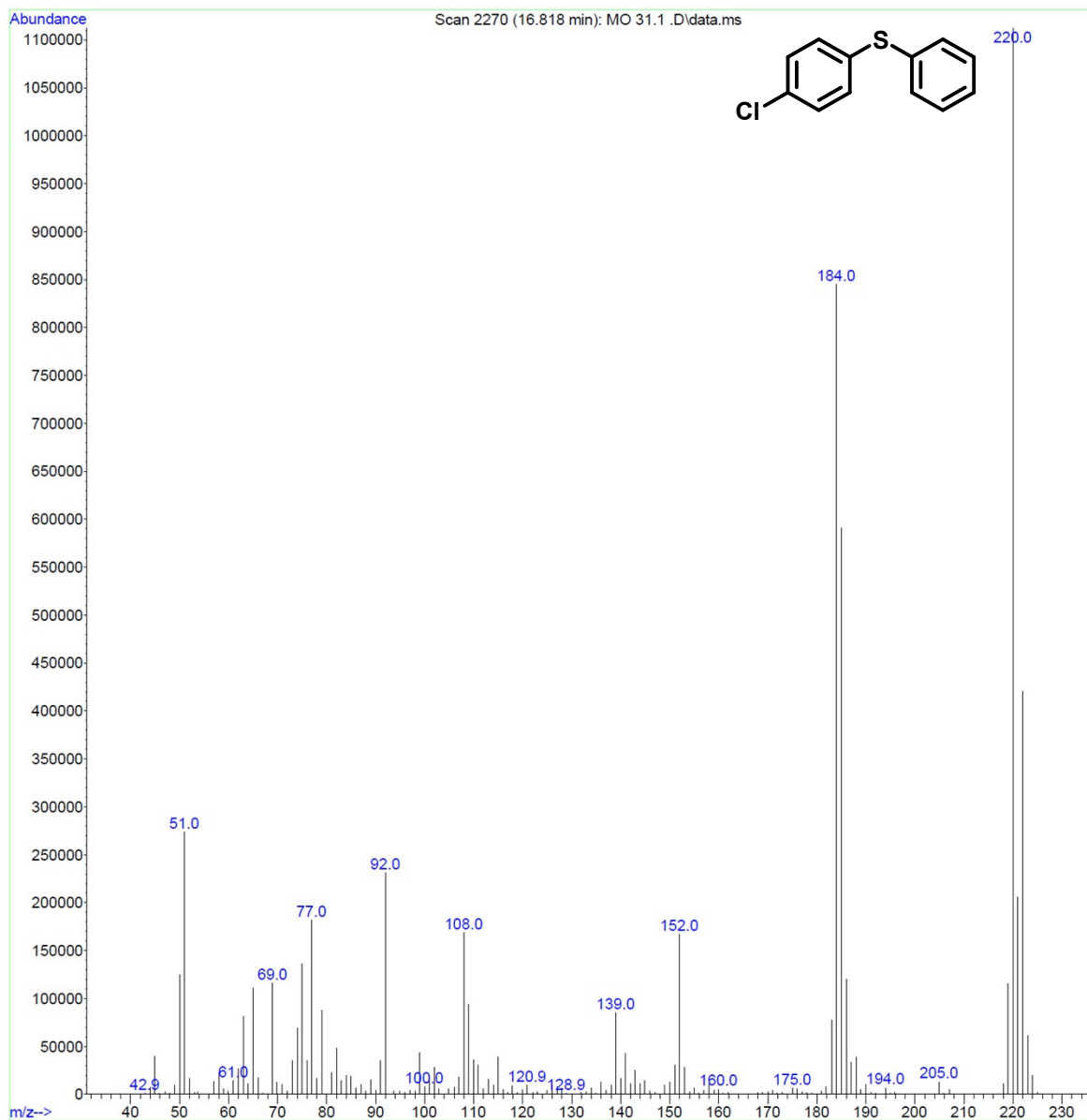


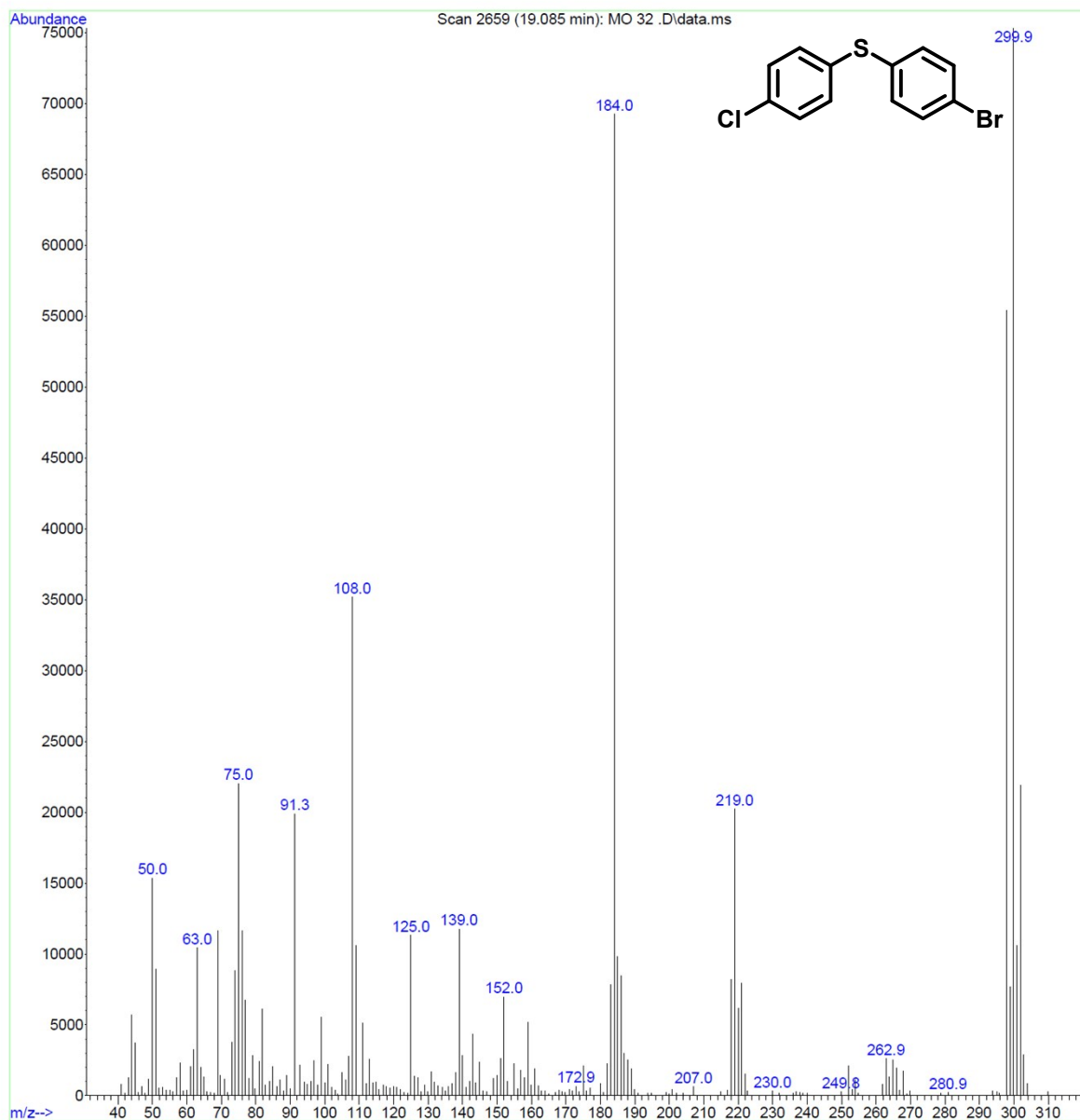


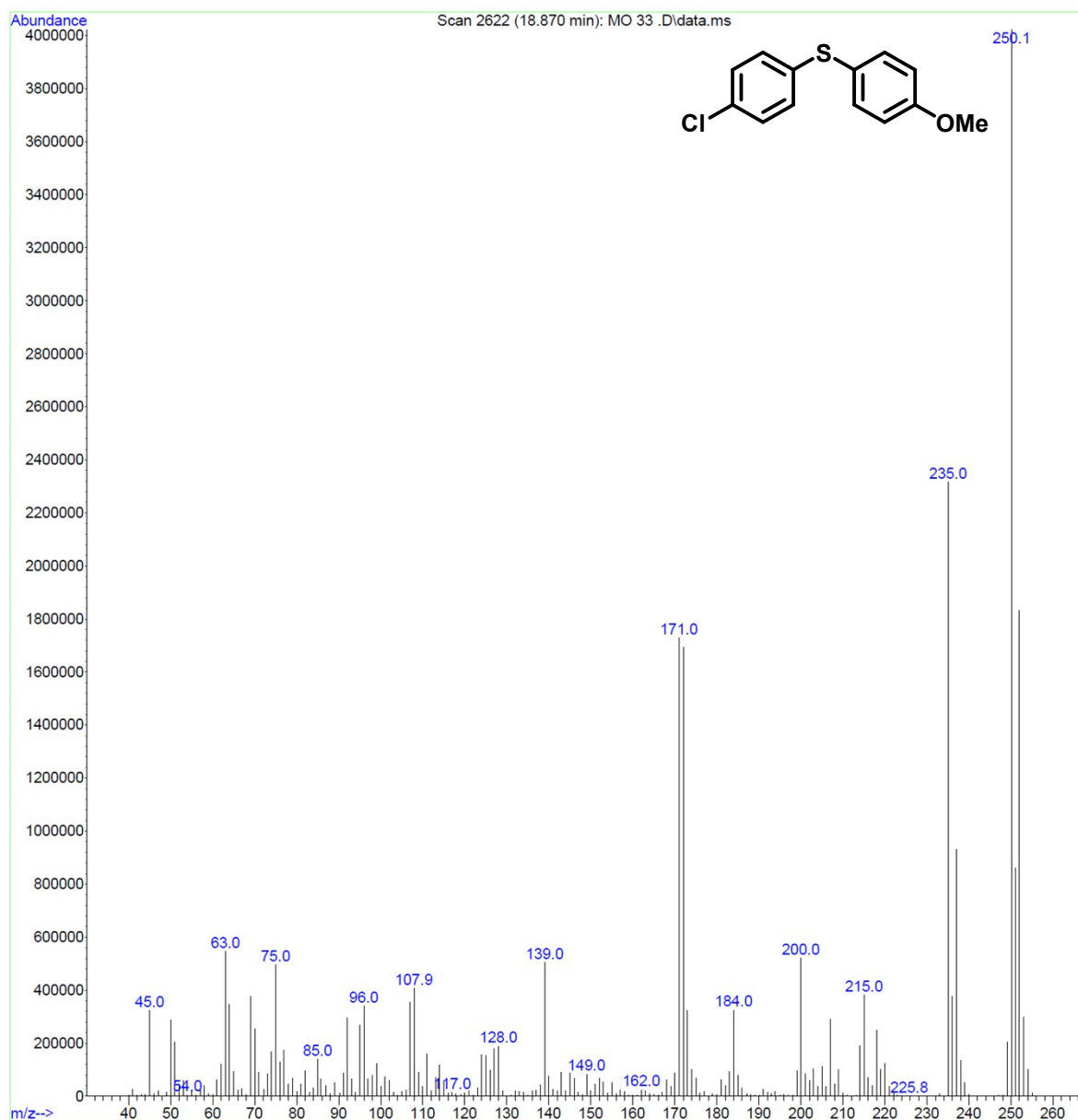


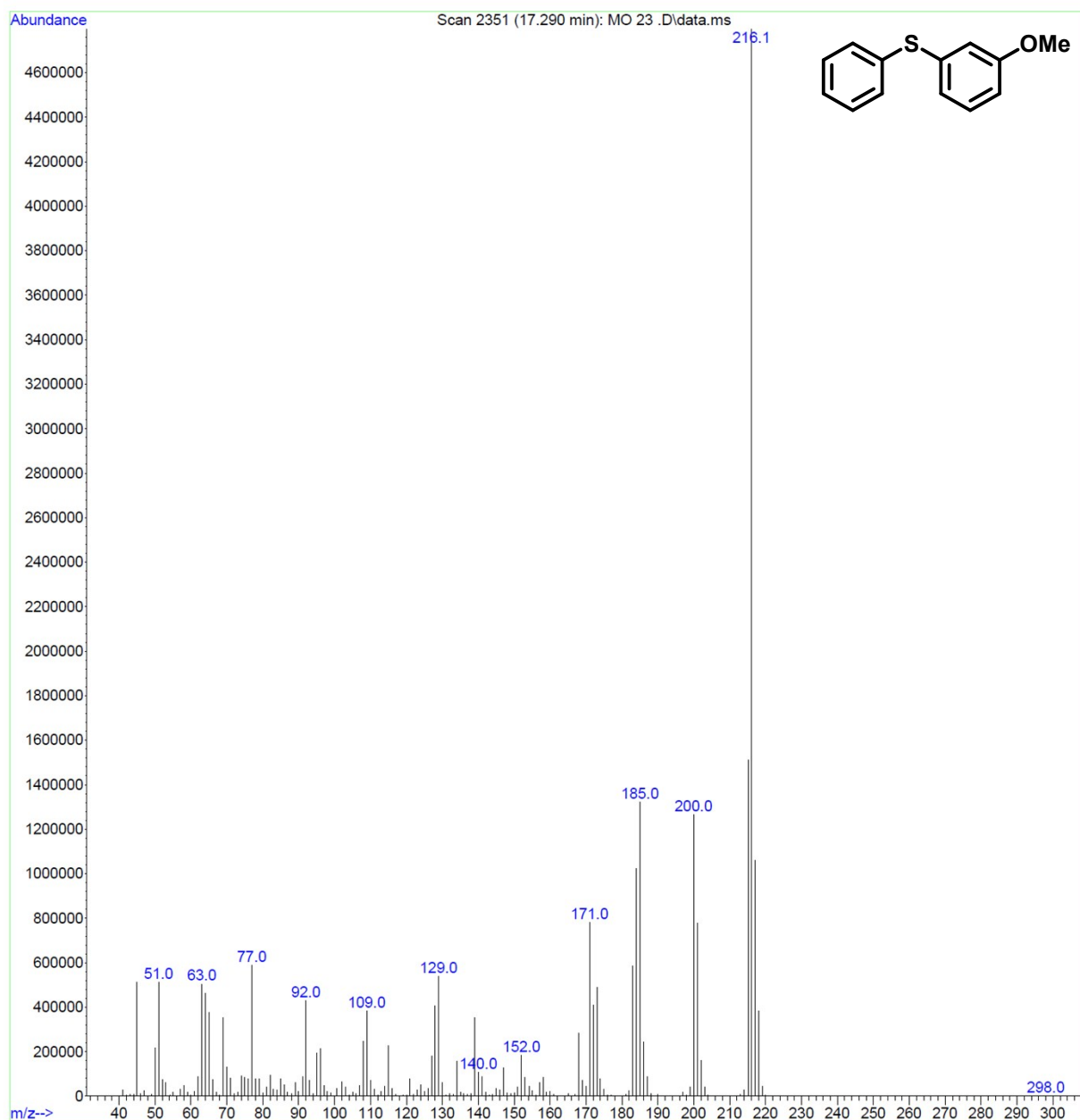


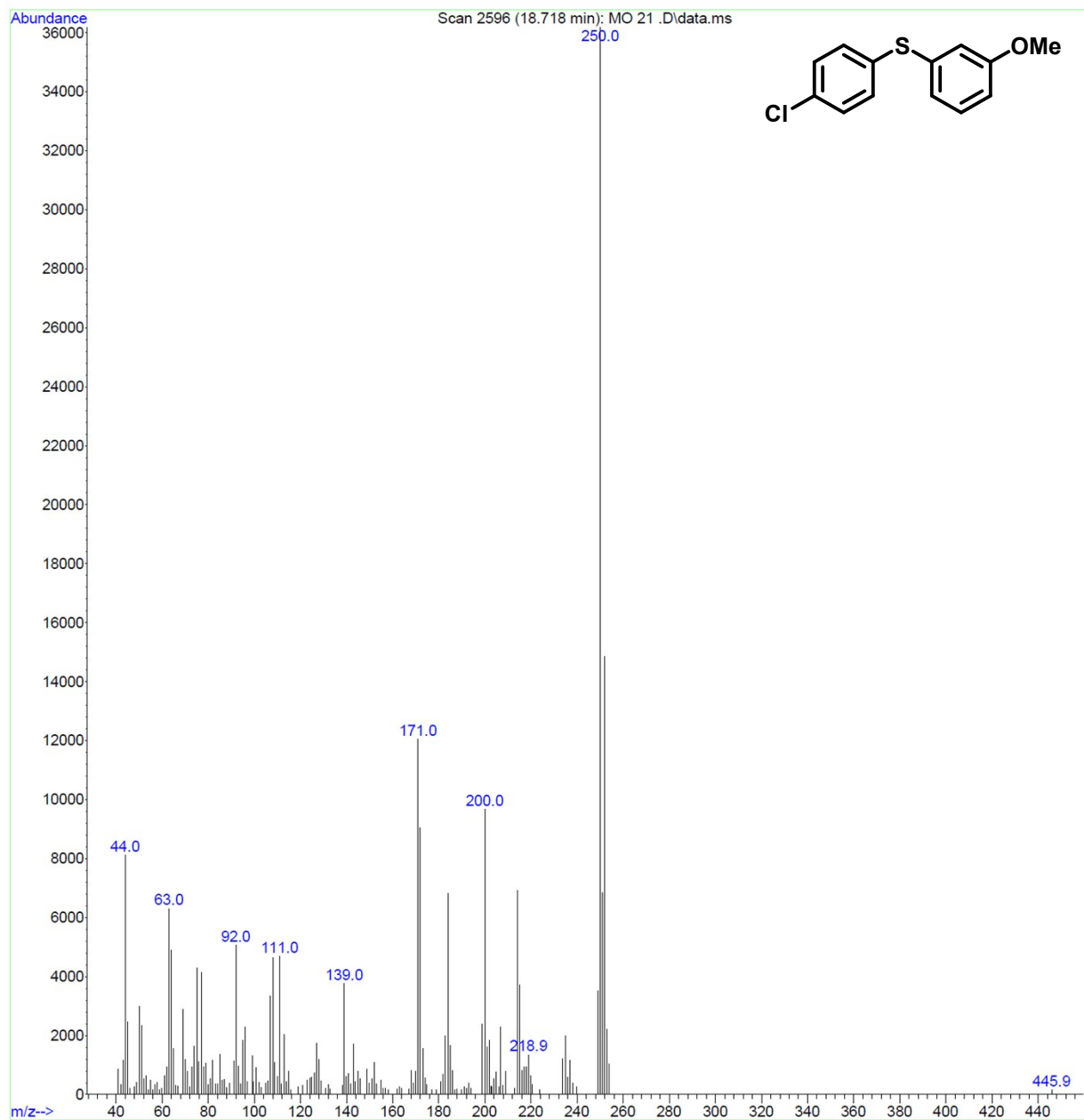


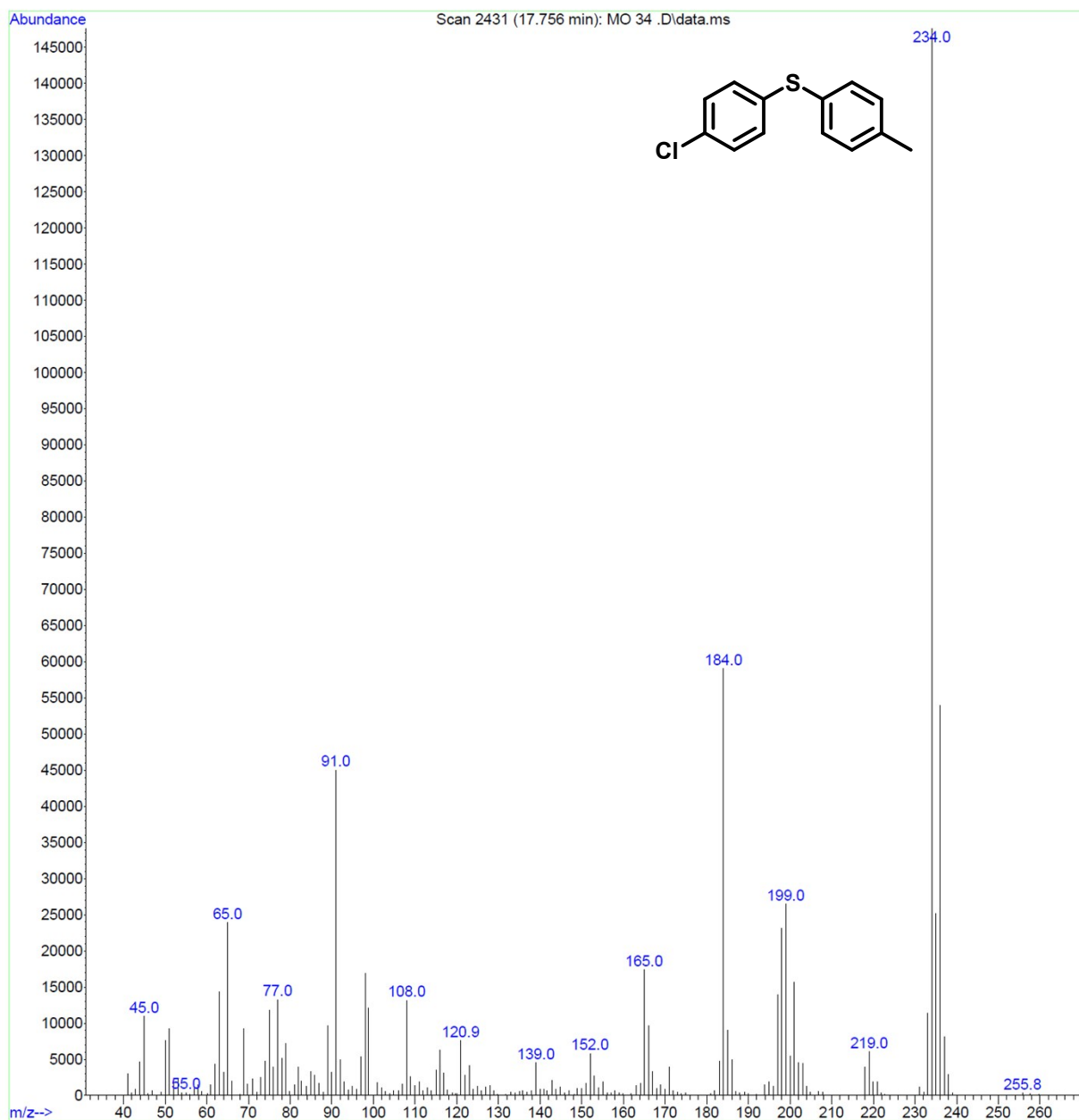


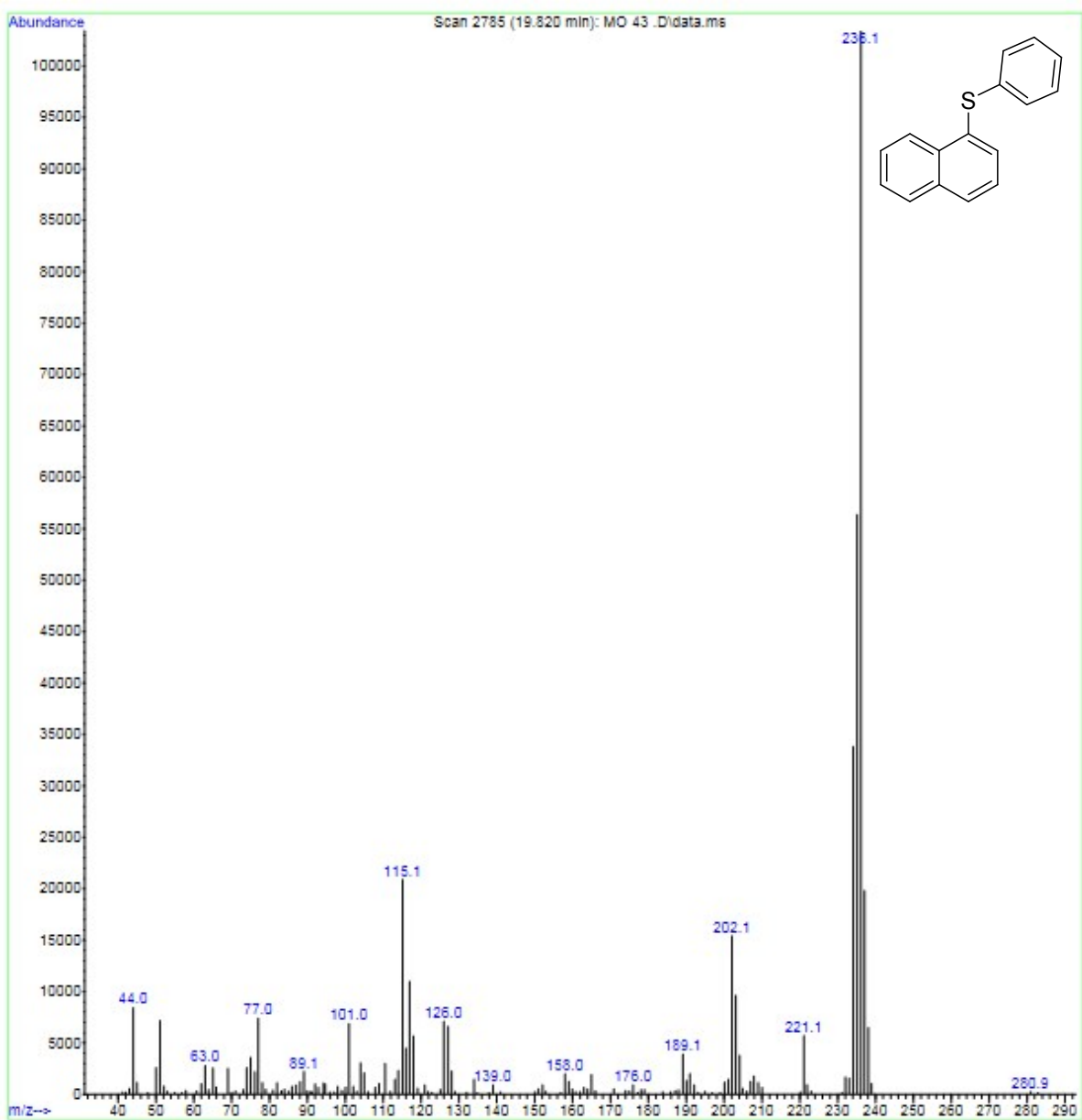


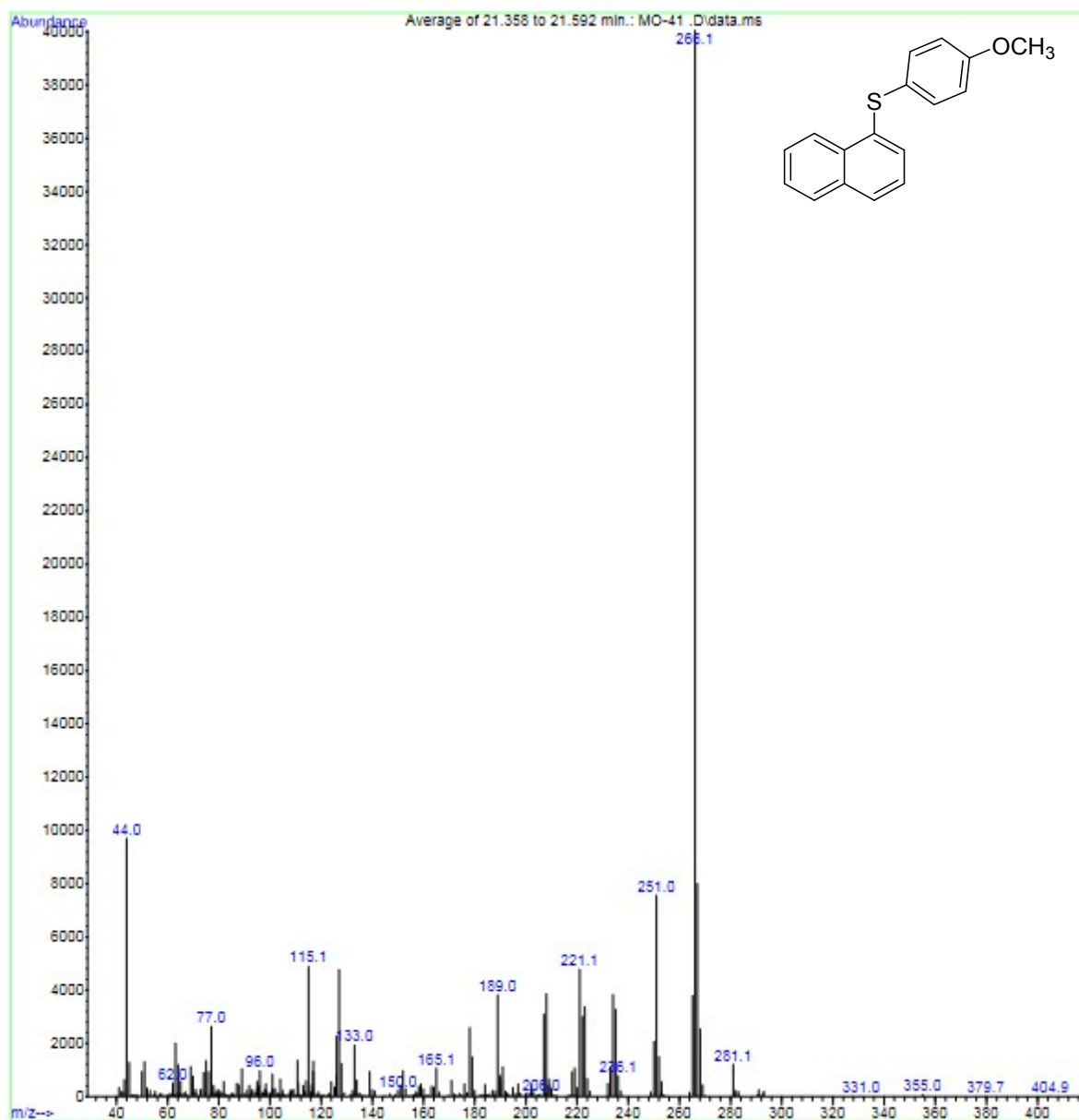




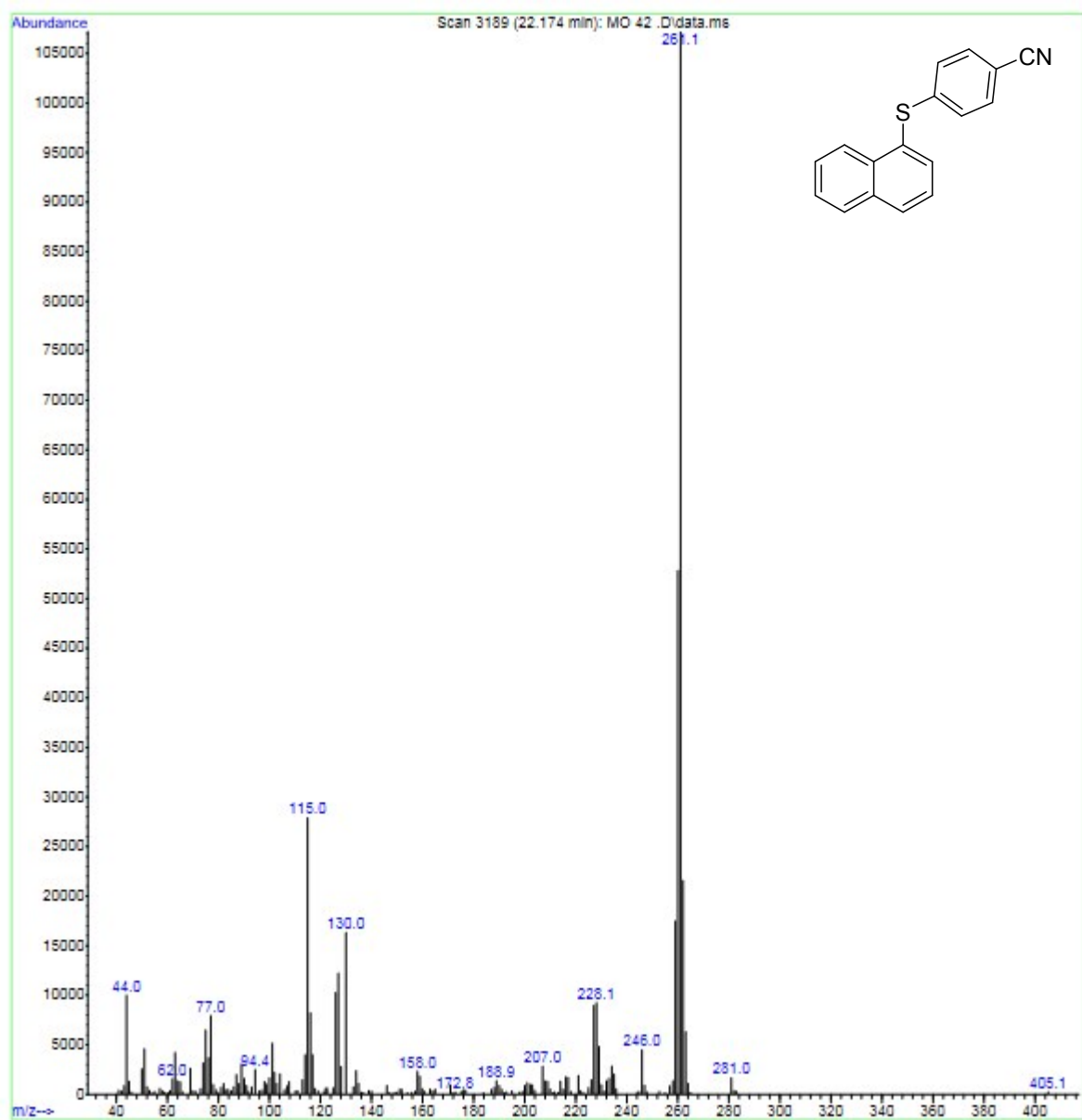


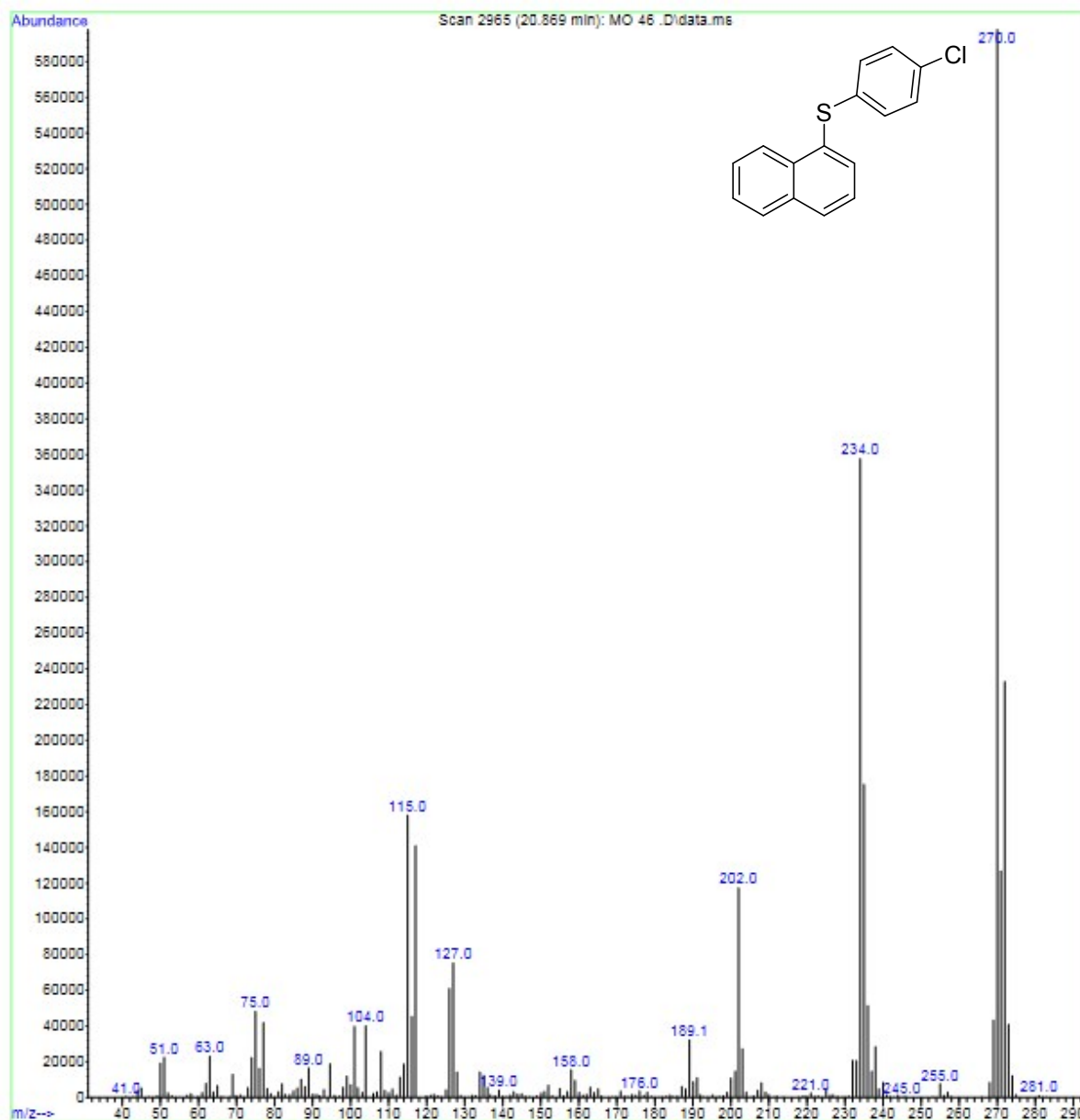












1. C. Wang, Z. Zhang, Y. Tu, Y. Li, J. Wu and J. Zhao, *J. Org. Chem.*, 2018, **83**, 2389-2394.
2. P. Guan, C. Cao, Y. Liu, Y. Li, P. He, Q. Chen, G. Liu and Y. Shi, *Tetrahedron Lett.*, 2012, **53**, 5987-5992.
3. Z.-B. Dong, M. Balkenhohl, E. Tan and P. Knochel, *Org. Lett.*, 2018, **20**, 7581-7584.
4. P. Anbarasan, H. Neumann and M. Beller, *Chem. Commun.*, 2011, **47**, 3233-3235.
5. K. Swapna, S. N. Murthy, M. T. Jyothi and Y. V. D. Nageswar, *Org. Biomol. Chem.*, 2011, **9**, 5989-5996.
6. J. A. Fernández-Salas, A. P. Pulis and D. J. Procter, *Chem. Commun.*, 2016, **52**, 12364-12367.
7. K. Kanemoto, Y. Sugimura, S. Shimizu, S. Yoshida and T. Hosoya, *Chem. Commun.*, 2017, **53**, 10640-10643.
8. S. Farzin, A. Rahimi, K. Amiri, A. Rostami and A. Rostami, *Appl. Organomet. Chem.*, 2018, **32**, e4409.
9. M. S. Oderinde, M. Frenette, D. W. Robbins, B. Aquila and J. W. Johannes, *J. Am. Chem. Soc.*, 2016, **138**, 1760-1763.
10. V. P. Reddy, K. Swapna, A. V. Kumar and K. R. Rao, *J. Org. Chem.*, 2009, **74**, 3189-3191.
11. X. Ren, S. Tang, L. Li, J. Li, H. Liang, G. Li, G. Yang, H. Li and B. Yuan, *J. Org. Chem.*, 2019, **84**, 8683-8690.
12. T. Taniguchi, T. Naka, M. Imoto, M. Takeda, T. Nakai, M. Mihara, T. Mizuno, A. Nomoto and A. Ogawa, *J. Org. Chem.*, 2017, **82**, 6647-6655.